




# Promyelinating drugs promote functional recovery in an autism spectrum disorder mouse model of Pitt–Hopkins syndrome

Joseph F. Bohlen,<sup>1</sup> Colin M. Cleary,<sup>2</sup> Debamitra Das,<sup>1</sup>  Srinidhi Rao Sripathy,<sup>1</sup> Norah Sadowski,<sup>1,3</sup> Gina Shim,<sup>1</sup> Rakaia F. Kenney,<sup>1</sup> Ingrid P. Buchler,<sup>1</sup> Tapasree Banerji,<sup>4</sup> Thomas S. Scanlan,<sup>4</sup> Daniel K. Mulkey<sup>2</sup> and Brady J. Maher<sup>1,3,5</sup>

Pitt–Hopkins syndrome is an autism spectrum disorder caused by autosomal dominant mutations in the human transcription factor 4 gene (*TCF4*). One pathobiological process caused by murine *Tcf4* mutation is a cell autonomous reduction in oligodendrocytes and myelination. In this study, we show that the promyelinating compounds, clemastine, sobetirome and Sob-AM2 are effective at restoring myelination defects in a Pitt–Hopkins syndrome mouse model. *In vitro*, clemastine treatment reduced excess oligodendrocyte precursor cells and normalized oligodendrocyte density. *In vivo*, 2-week intraperitoneal administration of clemastine also normalized oligodendrocyte precursor cell and oligodendrocyte density in the cortex of *Tcf4* mutant mice and appeared to increase the number of axons undergoing myelination, as EM imaging of the corpus callosum showed a significant increase in the proportion of uncompacted myelin and an overall reduction in the g-ratio. Importantly, this treatment paradigm resulted in functional rescue by improving electrophysiology and behaviour. To confirm behavioural rescue was achieved via enhancing myelination, we show that treatment with the thyroid hormone receptor agonist sobetirome or its brain penetrating prodrug Sob-AM2, was also effective at normalizing oligodendrocyte precursor cell and oligodendrocyte densities and behaviour in the Pitt–Hopkins syndrome mouse model. Together, these results provide preclinical evidence that promyelinating therapies may be beneficial in Pitt–Hopkins syndrome and potentially other neurodevelopmental disorders characterized by dysmyelination.

- 1 Lieber Institute for Brain Development, Johns Hopkins Medical Campus, Baltimore, MD 21205, USA
- 2 Department of Physiology and Neurobiology, University of Connecticut, Storrs, CT 06269, USA
- 3 Solomon H. Snyder Department of Neuroscience, Johns Hopkins University School of Medicine, Baltimore, MD 21205, USA
- 4 Department of Physiology & Pharmacology and Program in Chemical Biology, Oregon Health & Science University, Portland, OR 97239, USA
- 5 Department of Psychiatry and Behavioral Sciences, Johns Hopkins University School of Medicine, Baltimore, MD 21287, USA

Correspondence to: Brady J. Maher  
Lieber Institute for Brain Development  
855 N Wolfe St., Suite 300  
Johns Hopkins Medical Campus  
Baltimore, MD 21205, USA  
E-mail: brady.maher@libd.org

**Keywords:** myelination; Pitt–Hopkins syndrome; clemastine; ASD; sobetirome

Received May 31, 2022. Revised January 10, 2023. Accepted February 03, 2023. Advance access publication April 18, 2023

© The Author(s) 2023. Published by Oxford University Press on behalf of the Guarantors of Brain.

This is an Open Access article distributed under the terms of the Creative Commons Attribution-NonCommercial License (<https://creativecommons.org/licenses/by-nc/4.0/>), which permits non-commercial re-use, distribution, and reproduction in any medium, provided the original work is properly cited. For commercial re-use, please contact [journals.permissions@oup.com](mailto:journals.permissions@oup.com)

## Introduction

Autism spectrum disorder (ASD) is genetically heterogeneous with convergent symptomatology, suggesting the potential for common dysregulated pathways. Currently, there are no therapeutic interventions that address the core symptoms of ASD. One form of syndromic ASD caused by autosomal dominant mutations in the transcription factor 4 (TCF4; not TCF7L2/T-cell factor 4) gene results in Pitt–Hopkins syndrome (PTHS), a rare neurodevelopmental disorder (NDD) characterized by intellectual disability, failure to acquire language, deficits in motor learning, hyperventilation, gastrointestinal abnormalities and autistic behaviour.<sup>1</sup> Mouse models of PTHS consistently show behavioural deficits that approximate behavioural abnormalities observed in PTHS patients.<sup>2–5</sup> However, the pathophysiological mechanisms underlying these behavioural deficits are not completely understood.

Transcriptional profiling across five independent PTHS mouse models identified enrichment in differentially expressed genes related to myelination. This transcriptional profile was biologically validated, whereby *in vitro*, *ex vivo* and *in vivo* experiments demonstrated mutations in TCF4 resulted in a reduction in oligodendrocytes (OLs) in conjunction with dysmyelination related functional deficits.<sup>6</sup> Tcf4 is highly expressed in the entire OL lineage, and reductions in myelination due to Tcf4 mutations are cell autonomous.<sup>6–10</sup> Beyond PTHS, defects in the OL lineage are reported for a variety of ASD models and suggests this cell population may be a suitable target for therapeutic interventions. One well known promyelinating compound is clemastine fumarate, which is a well-studied, FDA-approved, first-generation antihistamine predominantly used in the treatment of allergic conditions.<sup>11</sup> Clemastine is a competitive antagonist at peripheral H1 receptors (H1R), blocking the actions of endogenous histamines, but its promyelination properties are thought to be through its muscarinic receptor 1 (M1R) activity.<sup>12–14</sup> Several studies have consistently shown clemastine promotes differentiation of oligodendrocyte progenitor cells (OPCs) into mature/myelinating OLs.<sup>13,15–17</sup> Another promyelination compound is sobetirome, a clinical-stage thyromimetic, and its CNS-penetrating prodrug Sob-AM2, which are effective at stimulating remyelination in several demyelination models.<sup>18</sup> Promoting myelination is an intriguing therapeutic approach for NDDs as the presence of mitotically active OPCs and the process of myelination occurs over the entire lifespan.<sup>19</sup>

In this study, we demonstrate that pharmacological enhancement of myelination with clemastine or sobetirome/Sob-AM2 are beneficial rescue approaches in a PTHS mouse model. We show administration of clemastine, both *in vitro* and *in vivo*, normalizes OPC and OL density, improves myelination and normalizes electrophysiological and behavioural deficits. Similarly, we show that treatment with sobetirome and Sob-AM2 are also effective at normalizing OPC and OL density and behavioural deficits. Together, these preclinical results indicate that promyelinating compounds may be a beneficial therapeutic approach for PTHS and other NDDs characterized by dysmyelination.

## Materials and methods

### Animals and tissue collection

The Tcf4<sup>+tr</sup> mouse model of PTHS is heterozygous for an allele encoding deletion of the DNA-binding domain of TCF4 (B6;129-TCF4tm1Zhu/J, stock number 013598, Jackson Laboratory).

This mouse colony was backcrossed for at least six generations, maintained by The Lieber Institute for Brain Developments Animal Facility on a 12-h light/dark cycle and fed *ad libitum*. Tcf4<sup>+tr</sup> mouse samples were matched with samples from Tcf4<sup>+/+</sup> littermates, and sex was randomly selected in each genotype and age group. All procedures were performed in accordance with the National Institutes of Health Guide for the Care and Use of Laboratory Animals and approved by the Johns Hopkins University School of Medicine's and University of Connecticut's Institutional Animal Care and Use Committee.

### Clemastine dosing regime

A dosing solution at concentration 1 mg/ml was generated by weighing out the appropriate quantity of clemastine fumarate (Sigma SML0445) in a septa seal vial. Then 5% DMA (dimethylacetamide, Sigma 271012) was added up to the total volume needed. The clemastine fumarate was completely dissolved in the DMA before the addition of saline to the appropriate volume. The vehicle consisted of 5% DMA in PBS. The mixture was shaken vigorously (vortex) and was ready for administration for intraperitoneal dosing at 10 ml/kg. The final pH was ~5. Animals were dosed every 24 h for 14 consecutive days at a dose of 10 mg/kg for clemastine or an equal volume of vehicle depending on the condition. The initial dosing was performed at postnatal Day 28 (P28) up until P42 when animals were then used for subsequent experiments.

### Sobetirome dosing regime

A dosing solution at concentration 1.0 mg/ml was generated by weighing out the appropriate quantity of sobetirome in a 15 ml falcon tube and resuspended in DMSO. A dose of 10 µM per day was used for *in vitro* studies (Sigma SML1900) following the previously described method of clemastine dosing *in vitro*. For *in vivo* intraperitoneal injections, we weighed out the appropriate quantity of Sob-AM2 (amide prodrug of sobetirome) and combined 1 ml of Kolliphor (C5135-500G), 1 ml of NMP (328634-100 ml) and 8 ml of Millipore water, and warmed at 37°C until a clear solution formed. Mice were dosed at 1.0 mg/kg/day for 14 days with either Sob-AM2 or NMP/Kolliphor solution (vehicle). Initial dosing was performed at P28 up until P42 when animals were then used for subsequent experiments.

### Primary oligodendrocyte progenitor cell and oligodendrocyte cultures

Primary OPC and OLs were obtained following a previous protocol.<sup>20</sup> In brief, the cortex of P2–P3 pups were dissociated and plated at a density of  $10.0 \times 10^3$  cells/cm<sup>2</sup> in a 96-well ibidi plate coated in 0.1% polyethyleneimine (PEI) and 0.5 µg/ml laminin. Cells were plated and maintained in OPC proliferation media consisting of 1× StemPro Neural supplement (Thermo Fisher Scientific, A1050801), 1× Anti-Anti (Thermo Fisher Scientific, 15240-096), 10 ng/ml of Human FGF-basic (Peprotech, 100-18B) and 30 ng/ml rhPDGF-AA (R&D systems, 221-AA), with a half media exchange on day *in vitro* 4 (DIV4). On DIV7 OL differentiation media was added (base media with removal of bFGF and rhPDGF-AA) and cells were differentiated into OLs with the addition of either DMSO (Sigma D8418 at 0.1%) as a vehicle or Clemastine/Sobetirome (Sigma SML0445 10 µM/Sigma SML1900 10 µM) with a media change every day until DIV14.

## Immunohistochemistry and immunocytochemistry

Cells were rinsed 1× with PBS and then fixed with 4% paraformaldehyde for 5 min, following fixation cells were rinsed 3× with PBS. Similarly, mice were perfused with 20–30 ml of 1× PBS, followed by 20–30 ml of 4% paraformaldehyde. Tissue was extracted and post-fixed in 4% paraformaldehyde on a rocker at 4°C overnight. For immunostaining, cells were rinsed three times with 0.04% Tween 20 (Sigma 655204) while tissue (P42 mouse) was rinsed three times with 0.4% Triton (Sigma X100). Cells were blocked in respective serum (10%) for 2 h at room temperature on an orbital shaker. Following the block, primary antibody was added in 2% serum in 0.04% Tween 20 for cells and 0.4% Triton-X 100 for tissue, and incubated overnight at 4°C. Following overnight incubation cells were rinsed three times with 0.04% Tween 20 or 0.4% Triton, respectively, before adding the secondary antibody to incubate at room temperature for 2 h. After incubation, cells were rinsed three times in respective buffers and counterstained with DAPI (Invitrogen™, D1306). Visualization was carried out on a ZEISS LSM 700 Confocal. Imaging and quantification were performed blind to genotypes and conditions/treatments. See [Supplementary Table 1](#) for a list of antibodies used.

## Transmission electron microscopy

After perfusion with a 0.1 M sodium cacodylate buffer, pH 7.2, containing 2% paraformaldehyde (freshly prepared from EM grade aqueous solution), 2% glutaraldehyde and 3 mM MgCl<sub>2</sub>, P42 mouse brains were kept overnight in fixative. The next day brains were dissected in fixative and rinsed with sodium cacodylate buffer. Samples were then post-fixed in reduced 2% osmium tetroxide, 1.6% potassium ferrocyanide in buffer (2 h) on ice in the dark. Following a dH<sub>2</sub>O rinse, samples were stained with 2% aqueous uranyl acetate (0.22 μm filtered, 1 h, dark), dehydrated in a graded series of ethanol, propylene oxide and embedded in Eponate 12 (Ted Pella) resin. Samples were polymerized at 60°C overnight. Thin sections, 60–90 nm, were cut with a diamond knife on the Reichert-Jung Ultracut E ultramicrotome and picked up with copper slot (1 × 2 mm) grids. Grids were stained with 2% uranyl acetate and observed with a Phillips CM120 transmission electron microscope (TEM) at 80 kV. Images were captured with an AMT XR80 CCD camera. Preparation of samples, TEM imaging and quantification was performed blind to genotypes. For quantification of the density of myelinated axons, we counted myelinated axons and divided them by the area of the image. Myelinated axons were then categorized as being either compacted or uncompacted on the basis of a visual inspection of the TEM image by a single experimenter who was blind to genotype and treatment condition. Examples of compacted and uncompacted myelinated axons are provided in [Fig. 3B](#). The proportion of compacted and uncompacted myelinated axons was the ratio of compacted or uncompacted myelin divided by the total number of myelinated axons. The g-ratio of myelinated axons was calculated as the ratio of the inner to the outer radius of the myelin sheath using ×20 000 magnification images from at least 150–200 axons from 10 images per animal.

## Electrophysiology

Acute coronal brain slices containing the corpus callosum (CC) were obtained from P39–P42 mice as previously described.<sup>21</sup> Artificial CSF was oxygenated (95% O<sub>2</sub> and 5% CO<sub>2</sub>) and contained (in mM): 125 NaCl, 25 NaHCO<sub>3</sub>, 1.25 NaH<sub>2</sub>PO<sub>4</sub>, 3 KCl, 25 dextrose, 1 MgCl<sub>2</sub> and 2 CaCl<sub>2</sub>, pH 7.3. A bipolar stimulating electrode was placed 500 μm

away from the midline and CC was stimulated with a 100 μs square pulse using 80% of the maximal stimulation intensity. The recording electrodes were fabricated from borosilicate glass (N51A, King Precision Glass, Inc.) to a resistance of 2–5 MΩ and placed at varying distances from the stimulating electrode in the contralateral CC. For compound action potential (CAP) recording, pipettes were filled with artificial CSF. Voltage signals were recorded with an Axopatch 200B amplifier (Molecular Devices) and were filtered at 2 kHz using a built in Bessel filter and digitized at 10 kHz. Data were acquired using Axograph on a Dell PC. For electrophysiology experiments, data collection and analysis were performed blind to the conditions of the experiment.

## Novel open field assay

Locomotor activity and anxiety was assessed using Noldus PhenoTyper cages as previously shown.<sup>22</sup> Each cage was outfitted with two sets of cameras; one on the ceiling that faced the platform (35 × 35 cm), and another pointed at the side of the cage. Mice were acclimated to the experimentation room in their home cages for at least 1 h. During acclimation, the Noldus EthoVision software was set up to track movement for a total of 30 min. After acclimation, mice were placed in the centre of the open field, opaque Plexiglas was placed on all four sides of the cage to obscure any visual cues and the trial was started in the EthoVision software. After 30 min, the trial ended and mice were placed back into their home cages. Noldus EthoVision software was used to determine distance travelled, time spent in centre and frequency of going to centre.

## Statistics

GraphPad Prism (GraphPad Software, San Diego, CA, USA) was used to conduct statistical analyses for immunohistochemical, ICC and behavioural experiments. Scipy stats package v.1.8.0 and Statsmodels package v.0.13.2 were used to conduct statistical analyses for EM and electrophysiology experiments. Data were analysed using either a two-way ANOVA, analysis of covariance (ANCOVA) or an unpaired t-test. All ANOVA main effects were followed by Tukey *post hoc* tests.

## Data availability

All data that support the findings of this study are available from the corresponding author, upon reasonable request.

## Results

### Clemastine enhances differentiation of oligodendrocyte progenitor cells *in vitro*

We first tested the effects of clemastine administration on OPCs *in vitro*. Previous studies indicate that clemastine is effective at promoting OPCs (PDGFR $\alpha$ +) in primary cultures to differentiate into OLs (MBP+).<sup>12,20</sup> Following a previously established protocol,<sup>20</sup> we dissociated and plated OPCs from both *Tcf4*<sup>+/+</sup> and *Tcf4*<sup>+/-</sup> mice onto 96-well plates in OPC proliferation media. OPCs were differentiated on DIV7 with OL differentiation media containing either clemastine (1 μM) or vehicle (DMSO), and fed every day with fresh media containing clemastine or vehicle before immunostaining on DIV14 ([Fig. 1A](#)). We performed blinded quantification of OPCs and OLs using antibodies against PDGFR $\alpha$  and MBP, respectively, and normalized our counts with the pan-OL marker OLIG2 ([Fig. 1B](#)). Consistent with previous observations,<sup>6</sup> *Tcf4*<sup>+/-</sup> cultures

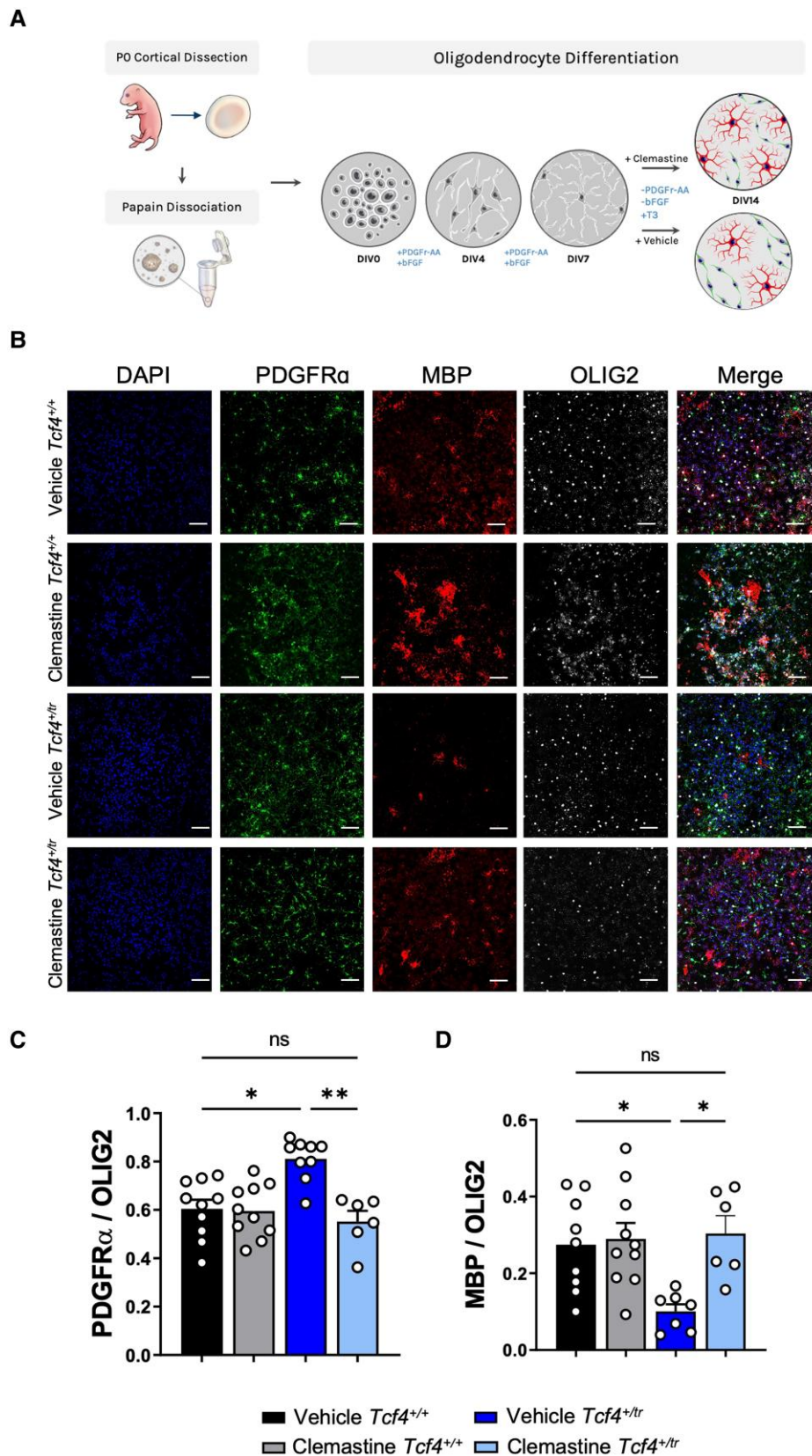


**Figure 1** Clemastine increases the proportion of OLs in *Tcf4*<sup>+tr</sup> cultures. (A) Graphical representation of the plating and dosing regimen. (B) Immunocytochemistry of DIV14 OPC/OL cultures following 7-day treatment with either vehicle (DMSO) or clemastine (1  $\mu$ M). Cultures stained for DAPI (blue, column 1), PDGFR $\alpha$  (green, column 2), MBP (red, column 3) and OLIG2 (grey, column 4). Scale bars = 50  $\mu$ m. (C) Summary plot showing the proportion of PDGFR $\alpha$ /OLIG2 cells is increased in vehicle-treated *Tcf4*<sup>+tr</sup> cultures compared to vehicle-treated *Tcf4*<sup>+/+</sup> cultures. The proportion of PDGFR $\alpha$ /OLIG2 cells is reduced in clemastine-treated *Tcf4*<sup>+tr</sup> cultures compared to vehicle-treated *Tcf4*<sup>+tr</sup> cultures [two-way ANOVA,  $n = 10$ –13 biologically independent animals/genotype,  $F(3,22) = 14.39$ ,  $P < 0.0001$ , data are presented as mean values  $\pm$  SEM]. (D) Summary plot showing the proportion of MBP/OLIG2 cells is decreased in vehicle-treated *Tcf4*<sup>+tr</sup> cultures compared to vehicle-treated *Tcf4*<sup>+/+</sup> cultures. The proportion of MBP/OLIG2 cells is increased in clemastine-treated *Tcf4*<sup>+tr</sup> cultures compared to vehicle-treated *Tcf4*<sup>+/+</sup> cultures [two-way ANOVA,  $n = 11$ –13 biologically independent animals/genotype,  $F(3,19) = 5.966$ ,  $P = 0.0048$  data are presented as mean values  $\pm$  SEM]. \* $P < 0.05$ , \*\* $P < 0.01$ .

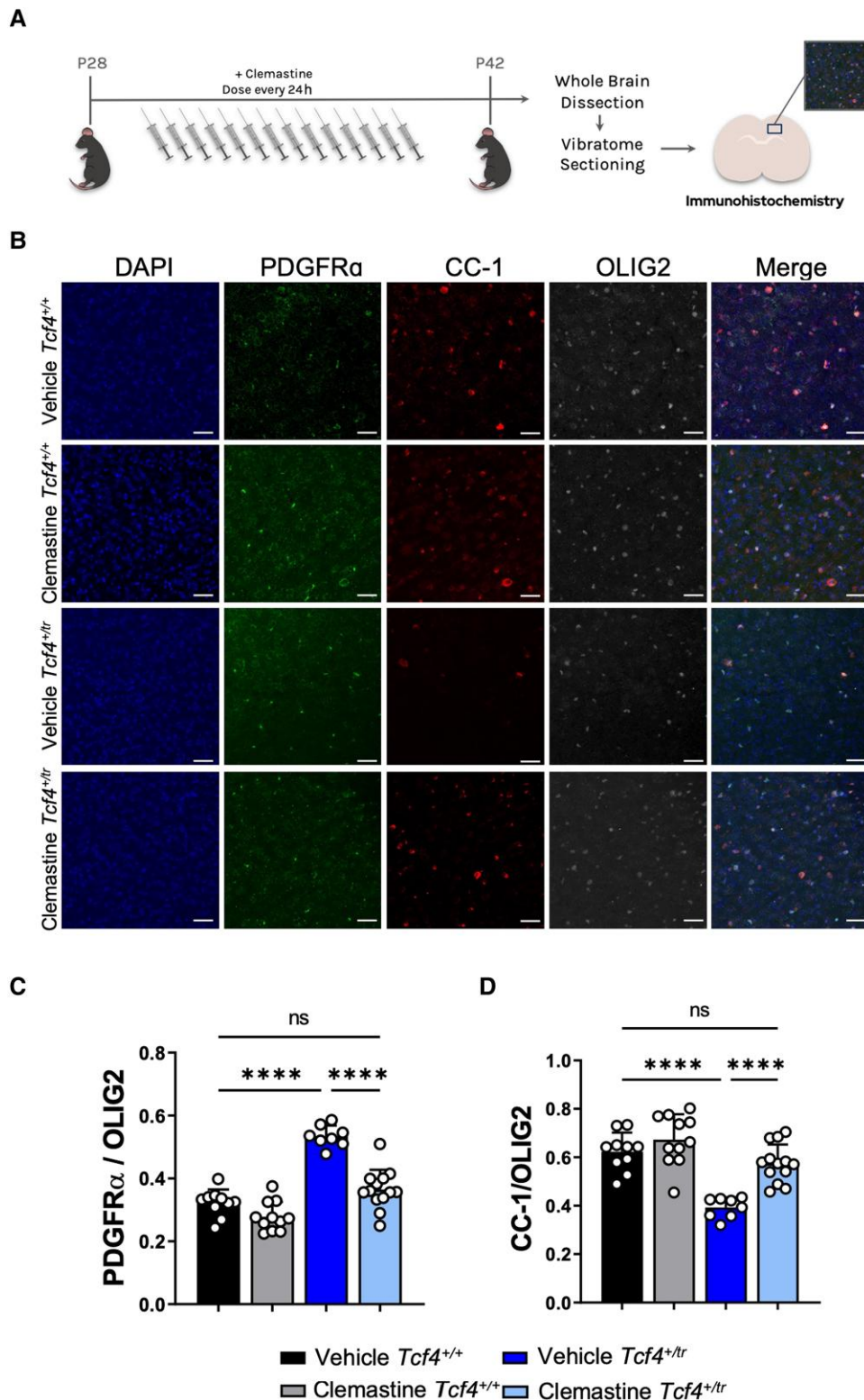


**Figure 2** *In vivo* clemastine treatment increases the proportion of OLS in *Tcf4*<sup>tr/tr</sup> mice. (A) Graphical representation of the dosing regime *in vivo*. (B) Immunohistochemistry of OPC/OL in 55  $\mu$ m-thick tissue sections following 14-day treatment of either vehicle (DMSO) or clemastine. Tissue stained for DAPI (blue, column 1), PDGFR $\alpha$  (green, column 2), MBP (red, column 3) and OLIG2 (grey, column 4). Scale bars = 50  $\mu$ m. (C) Summary plot showing the proportion of PDGFR $\alpha$ /OLIG2 cells is increased in vehicle-treated *Tcf4*<sup>tr/tr</sup> mice compared to vehicle-treated *Tcf4*<sup>+/+</sup> mice. The proportion of PDGFR $\alpha$ /OLIG2 cells is reduced in clemastine-treated *Tcf4*<sup>tr/tr</sup> mice compared to vehicle-treated *Tcf4*<sup>tr/tr</sup> mice [two-way ANOVA,  $n = 10$ –13 biologically independent animals/genotype,  $F(3,23) = 58.28$ ,  $P < 0.0001$ , data are presented as mean values  $\pm$  SEM]. (D) Summary plot showing the proportion of MBP/OLIG2 cells is decreased in vehicle-treated *Tcf4*<sup>tr/tr</sup> mice compared to vehicle-treated *Tcf4*<sup>+/+</sup> mice. The proportion of MBP/OLIG2 cells is increased in clemastine-treated *Tcf4*<sup>tr/tr</sup> mice compared to vehicle-treated *Tcf4*<sup>tr/tr</sup> mice [two-way ANOVA,  $n = 10$ –13 biologically independent animals/genotype,  $F(3,23) = 26.20$ ,  $P < 0.0001$ , data are presented as mean values  $\pm$  SEM]. \*\*\*\* $P < 0.0001$ .

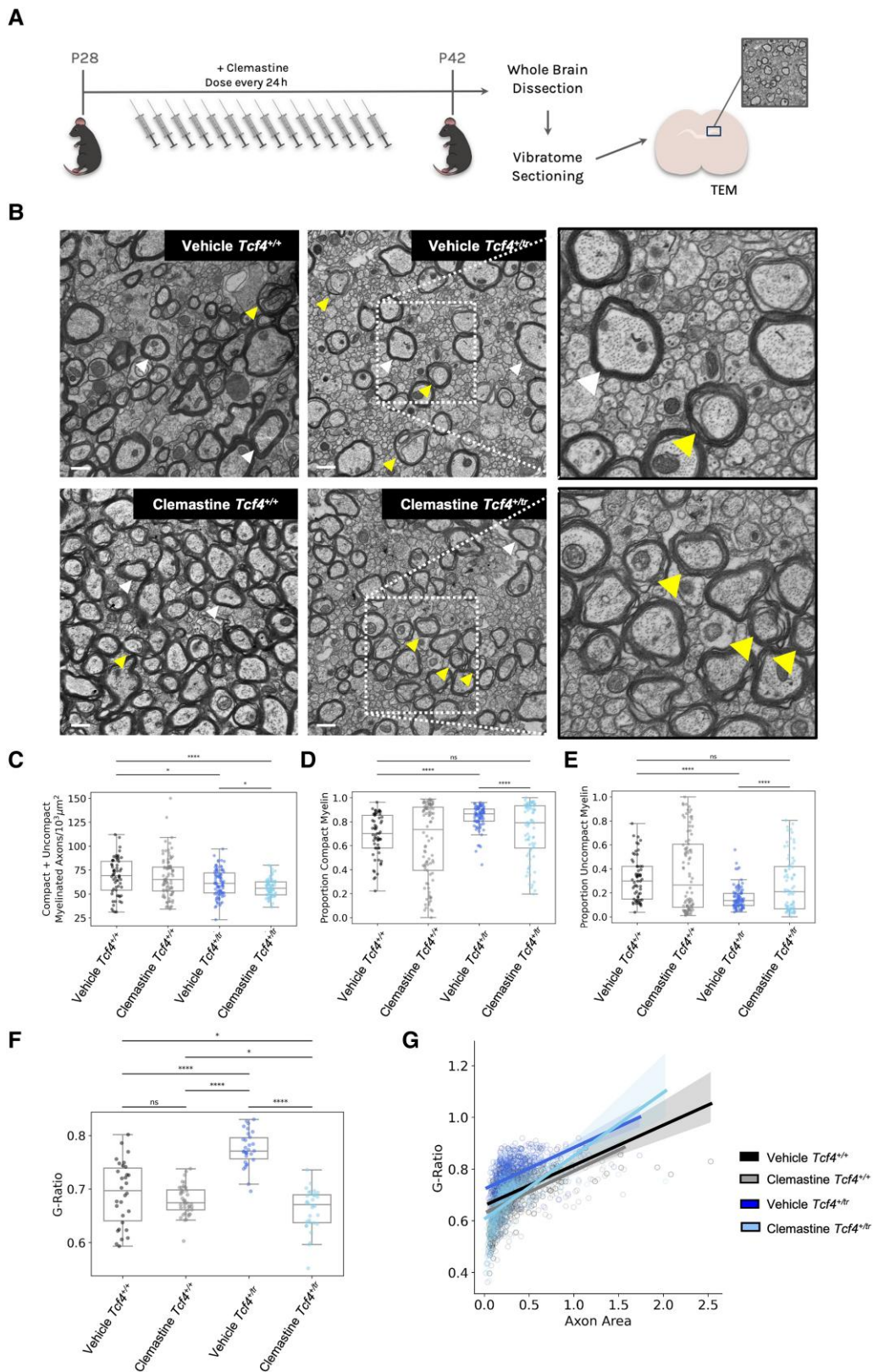


**Figure 3** Clemastine increases the proportion of uncompacted myelinated axons and reduces the g-ratio in the CC of the  $Tcf4^{+/tr}$  mice. (A) Graphical representation of the dosing regime and subsequent TEM. (B) Representative electron micrographs of the CC from vehicle and clemastine-treated  $Tcf4^{+/+}$  and  $Tcf4^{+/tr}$  mice. Arrowheads indicate compacted (white) and uncompacted (yellow) myelin designations. Scale bars = 500 nm. (C) Summary plot showing the density of compacted + uncompacted myelinated axons across all images for all conditions showing  $Tcf4^{+/tr}$  mice show a reduction in total myelin compared to  $Tcf4^{+/+}$  littermates. The density of myelinated axons was reduced in vehicle-treated  $Tcf4^{+/tr}$  mice compared to vehicle-treated  $Tcf4^{+/+}$  littermates (two-way ANOVA biologically independent animals/genotype  $F=1.54$ ,  $P=0.22$ ). (D) Proportion of compacted myelin per image

(Continued)

treated with vehicle showed a significant decrease in OLs (MBP+/OLIG2+) along with a significant increase in OPCs (PDGFR $\alpha$ +/OLIG2+) when compared to *Tcf4*<sup>+/+</sup> littermate controls (Fig. 1C and D). Clemastine treatment resulted in a significant reduction in OPCs and an increase in OLs when compared to vehicle-treated *Tcf4*<sup>+/-</sup> cells (Fig. 1C and D). These data indicate clemastine is effective at overcoming OPC deficits related to loss of TCF4 by promoting differentiation of OPCs into OLs and thereby normalizing the OL population to similar proportions of OPCs and OLs observed in *Tcf4*<sup>+/+</sup> cultures.

### Clemastine increases the number of oligodendrocytes *in vivo*

Next, we assessed the effectiveness of clemastine *in vivo* by dosing *Tcf4*<sup>+/-</sup> mice and *Tcf4*<sup>+/+</sup> littermates intraperitoneally with either clemastine (10 mg/kg) or vehicle for 2 weeks followed by blinded immunohistochemical quantification in the cortex above the CC in anatomically equivalent coronal brain sections containing dorsal hippocampus (Fig. 2A). Consistent with prior results,<sup>6</sup> vehicle-treated *Tcf4*<sup>+/-</sup> mice showed fewer OLs (CC1+/OLIG2+) and more OPCs (PDGFR $\alpha$ +/OLIG2+) when compared to vehicle-treated *Tcf4*<sup>+/+</sup> littermates (Fig. 2C and D). Similar to our *in vitro* data, clemastine-treated *Tcf4*<sup>+/-</sup> mice showed a significant increase in OLs that coincided with a significant decrease in OPCs when compared to their vehicle-treated *Tcf4*<sup>+/+</sup> littermates (Fig. 2C and D). Clemastine had no effect on the total number of OLIG2 positive cells across all conditions for both *in vitro* or *in vivo* assays (Supplementary Fig. 1), which indicates clemastine treatment is promoting OPCs to differentiate into OLs. We also investigated the long-term outcome of our 2-week clemastine treatment. After dosing animals for 2 weeks, we halted administration of clemastine at P42 and then collected samples at P90. Remarkably, the OL population remained elevated in clemastine-treated *Tcf4*<sup>+/-</sup> mice compared to vehicle-treated *Tcf4*<sup>+/+</sup> littermates, while effects on the OPC population diminished (Supplementary Fig. 2), suggesting that OLs created in response to clemastine are maintained, but the OPC population continues to abnormally expand due to the mutation in *Tcf4*. Together, these data indicate clemastine is effective *in vivo* at promoting OPCs to differentiate into OLs in a *Tcf4*<sup>+/-</sup> background, thereby normalizing the OL population to *Tcf4*<sup>+/+</sup> levels.

### Clemastine increases myelination activity and overall myelination in *Tcf4*<sup>+/-</sup> mice

To visualize myelination, we used TEM in both *Tcf4*<sup>+/+</sup> and *Tcf4*<sup>+/-</sup> littermates that had been dosed with either vehicle or clemastine (Fig. 3A). Blinded to genotype and condition, TEM images were taken on the CC directly above the hippocampus from anatomically equivalent tissue sections in littermates. Following blinded quantification, we replicated our previous observation that *Tcf4* mutation leads to a reduction in myelinated axons in the CC (Fig. 3B and C).

However, we observed that the 2-week clemastine treatment in *Tcf4*<sup>+/-</sup> mice was unable to restore the levels of total myelinated axon (compacted + uncompact) density to those observed in *Tcf4*<sup>+/+</sup> mice (Fig. 3B and C). We next quantified the proportion of compacted or uncompact myelinated axons and observed that the balance between myelinated axons (compacted) and ongoing myelination (uncompact) was different between vehicle-treated *Tcf4*<sup>+/-</sup> mice and vehicle-treated *Tcf4*<sup>+/+</sup> littermates (Fig. 3D and E), suggesting that the active process of myelination was reduced in *Tcf4*<sup>+/-</sup> mice. Notably, we observed that clemastine treatment significantly shifted the proportion of uncompact myelin in *Tcf4*<sup>+/-</sup> mice compared to vehicle-treated *Tcf4*<sup>+/-</sup> mice, and normalized the proportion of uncompact myelin to levels observed in vehicle-treated *Tcf4*<sup>+/+</sup> mice (Fig. 3E), suggesting clemastine treatment is promoting the generation of newly myelinated axons in the CC. Next, we quantified g-ratios and observed *Tcf4*<sup>+/-</sup> mice showed a significant increase in g-ratios compared to myelinated axons in *Tcf4*<sup>+/+</sup> mice (Fig. 3F and G), suggesting that *Tcf4*<sup>+/-</sup> mice have reduced myelin thickness. Following clemastine treatment, the g-ratio from myelinated axons in *Tcf4*<sup>+/-</sup> mice was significantly reduced compared to vehicle-treated *Tcf4*<sup>+/-</sup> mice (Fig. 3F and G), further demonstrating the promyelinating capabilities of clemastine treatment in *Tcf4*<sup>+/-</sup> mice (Fig. 3F and G). Last, we quantified the proportion of pre-myelinating OLs (BCAS1+) in vehicle and clemastine-treated *Tcf4*<sup>+/+</sup> and *Tcf4*<sup>+/-</sup> mice. Consistent with our EM data, we observed a significant reduction in BCAS1 positive OLs in vehicle-treated *Tcf4*<sup>+/-</sup> mice compared to vehicle-treated *Tcf4*<sup>+/+</sup> mice and this effect of genotype was rescued by clemastine treatment (Fig. 4A and B). Considering these data together with our *in vivo* and *in vitro* immunocytochemistry data, we conclude that this relatively short clemastine treatment effectively enhanced the production of OLs capable of generating new myelin ensheathment of axons.

### Clemastine rescues electrophysiological deficits in *Tcf4*<sup>+/-</sup> mice

We next determined whether clemastine's effect on the OL population was effective at normalizing physiology in *Tcf4*<sup>+/-</sup> mice. We measured the propagation of CAPs in the CC in acute brain slices from *Tcf4*<sup>+/+</sup> and *Tcf4*<sup>+/-</sup> mice. CAPs were evoked by a bipolar stimulating electrode and recorded by a field electrode placed at varying distances across the CC and the amplitude of N1 and N2 peaks was quantified (Fig. 5A). The N1 and N2 peaks represent CAPs travelling down myelinated and unmyelinated axons, respectively,<sup>23</sup> and we previously showed the N1/N2 ratio was significantly reduced in *Tcf4*<sup>+/-</sup> mice.<sup>6</sup> Two-week clemastine treatment of *Tcf4*<sup>+/-</sup> mice was effective at increasing the N1/N2 ratio compared to vehicle-treated *Tcf4*<sup>+/-</sup> littermates (Fig. 5C and D). Thus, indicating continued myelination in response to clemastine was effective at improving the physiological function of the CC in the PTHS mouse model.

#### Figure 3 Continued

showing a smaller proportion of compacted myelin in vehicle-treated *Tcf4*<sup>+/-</sup> mice compared to vehicle-treated *Tcf4*<sup>+/+</sup> mice. The proportion of compact myelin was reduced in clemastine-treated *Tcf4*<sup>+/-</sup> mice compared to vehicle-treated *Tcf4*<sup>+/-</sup> mice (two-way ANOVA biologically independent animals/genotype  $F = 1.24$ ,  $P = 0.26$ ). (E) Proportion of uncompact myelin per image showing a smaller proportion of compacted myelin in vehicle-treated *Tcf4*<sup>+/-</sup> mice compared to vehicle-treated *Tcf4*<sup>+/+</sup> mice. The proportion of compacted myelin was increased in clemastine *Tcf4*<sup>+/-</sup> mice compared to vehicle-treated *Tcf4*<sup>+/-</sup> mice (two-way ANOVA biologically independent animals/genotype  $F = 1.24$ ,  $P = 0.26$ ). (F) Summary plot showing the g-ratios across all conditions, analysis of three to four animals per condition (100–200 myelinated axons per animal collected). The g-ratio was elevated in vehicle-treated *Tcf4*<sup>+/-</sup> mice compared to vehicle-treated *Tcf4*<sup>+/+</sup> mice. The g-ratio was reduced in clemastine-treated *Tcf4*<sup>+/-</sup> mice compared to vehicle-treated *Tcf4*<sup>+/-</sup> mice (two-way ANOVA biologically independent animals/genotype  $F = 49.16$ ,  $P < 0.0001$ ). (G) Distribution of g-ratios for all conditions (ANCOVA  $F = 244.5$ ,  $P$ -value  $< 0.0001$ ). Centre values represent the mean and error bars are SEM, \* $P < 0.05$ , \*\*\*\* $P < 0.0001$ .

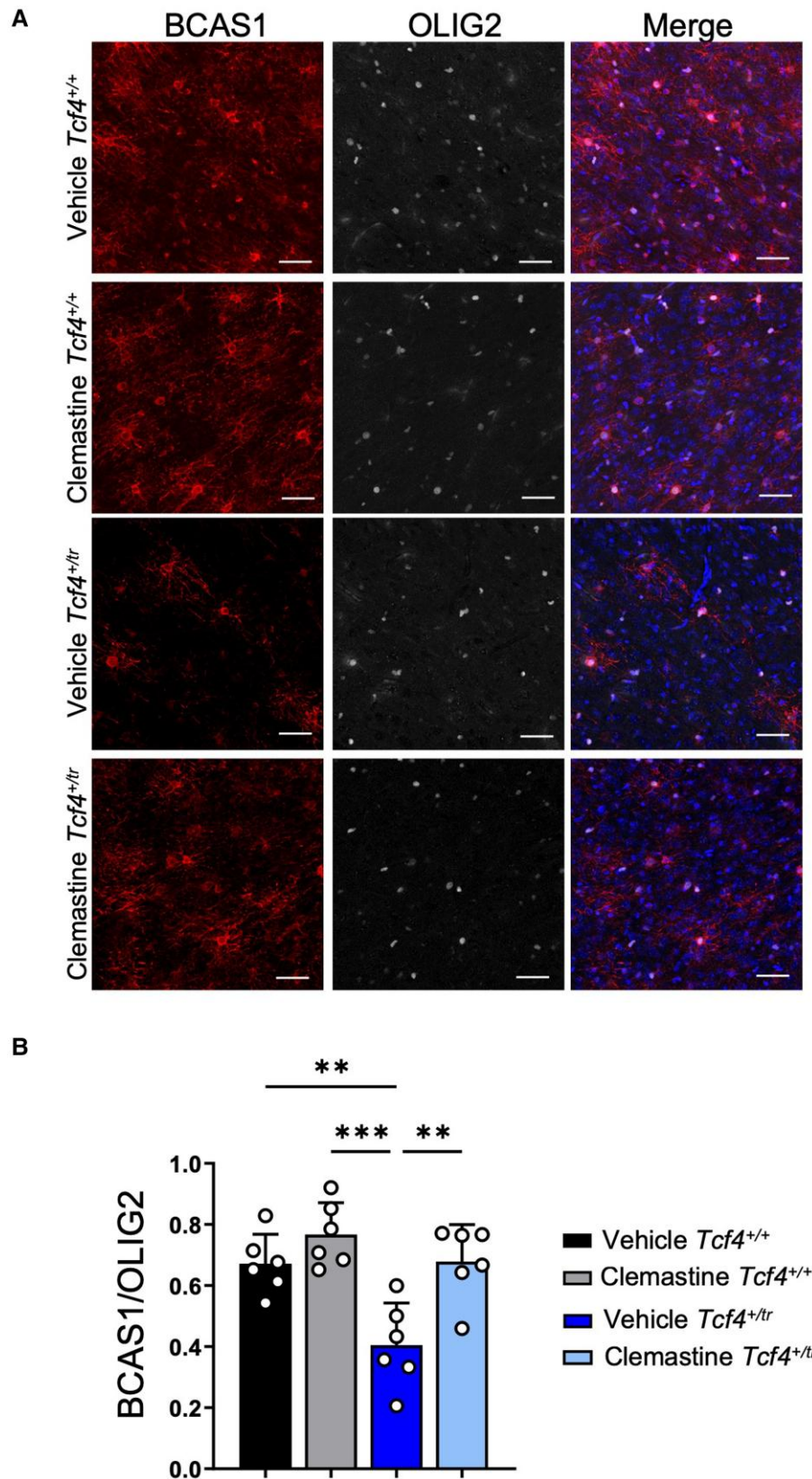


**Figure 4** Clemastine increases the number of pre-myelinating OLs in *Tcf4*<sup>+tr</sup> mice. (A) Immunohistochemistry of OPC/OL in 55  $\mu$ M tissue slices following 14 days of either vehicle (DMSO) or clemastine administration. Tissue stained for DAPI (blue), BCAS1 (red, column 1) and OLIG2 (grey, column 2). Scale bars = 50  $\mu$ m. (B) Summary plot showing a reduction in proportion of BCAS1/OLIG2 positive cells in vehicle-treated *Tcf4*<sup>+tr</sup> mice compared to vehicle-treated *Tcf4*<sup>+/+</sup> mice. The proportion of BCAS1/OLIG2 positive cells was increased in clemastine-treated *Tcf4*<sup>+tr</sup> mice compared to vehicle-treated *Tcf4*<sup>+tr</sup> mice [two-way ANOVA,  $n = 6$  biologically independent animals/genotype  $F(1,5) = 18.73$ ,  $P < 0.0001$ , data are presented as mean values  $\pm$  SEM]. \*\* $P < 0.01$ , \*\*\* $P < 0.001$ .



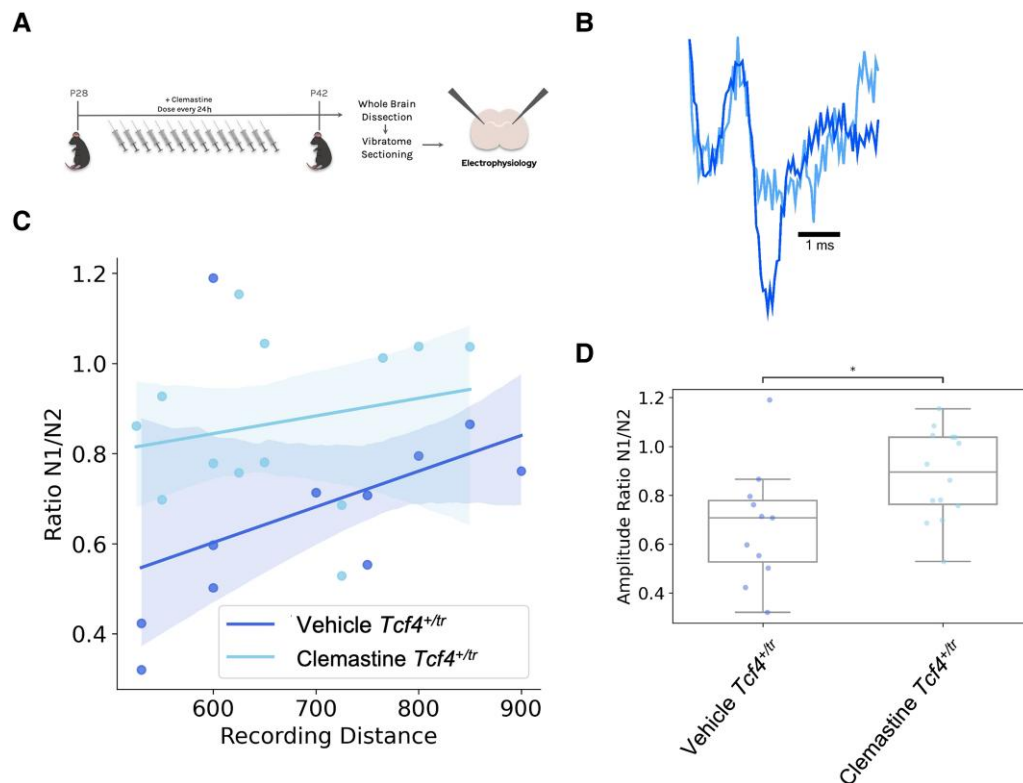


**Figure 5** Clemastine rescues electrophysiological deficits in the  $Tcf4^{+tr}$  mice. (A) Graphical representation of the dosing regime and subsequent electrophysiology. (B) Representative electrophysiology traces of evoked CAPs recorded in the CC from vehicle  $Tcf4^{+tr}$  and clemastine-treated  $Tcf4^{+tr}$  mice. N1 represents action potentials travelling down myelinated axons and N2 represents action potentials travelling down unmyelinated axons. Example traces are normalized by the N1 peak. (C) Linear regression fit of the N1/N2 ratio at its respective recording distance (ANCOVA  $F = 6.43$ ,  $P = 0.019$ ). (D) The proportion of action potentials travelling down myelinated axons was consistently reduced in vehicle-treated  $Tcf4^{+tr}$  mice compared to clemastine-treated  $Tcf4^{+tr}$  mice ( $P = 0.034$ ).

### Clemastine rescues behavioural deficits in $Tcf4^{+tr}$ mice

Given the clemastine-dependent increases in the OL population and rescue of electrophysiology in  $Tcf4^{+tr}$  mice, we wanted to determine whether these changes could ameliorate behavioural deficits in these mice. It was previously shown that a variety of PTHS mouse models display consistent behavioural deficits, including hyperlocomotion and reduced anxiety in the open field among others.<sup>2,5,24</sup> Therefore, we treated  $Tcf4^{+tr}$  mice and  $Tcf4^{+/+}$  littermates with clemastine for 14 days and then assayed their behaviour in the open field (Fig. 6A). Vehicle-treated  $Tcf4^{+tr}$  animals exhibited an overall greater distance travelled and increased frequency of entering the centre of the field (inversely related to anxiety) (Fig. 6B and C). Remarkably, clemastine-treated  $Tcf4^{+tr}$  mice showed a significant reduction in total distance travelled and diminished frequency of entering the centre of the field, to the level observed in vehicle  $Tcf4^{+/+}$  mice (Fig. 6B and C). These data indicate that clemastine treatment is effective at normalizing hyperlocomotion and anxiety phenotypes in the PTHS mouse model.

### Sobetirome rescues oligodendrocyte density and behaviour in $Tcf4^{+tr}$ mice

The polypharmacology of clemastine makes it difficult to ascertain whether its behavioural normalization in the PTHS mouse model results from its promyelinating capabilities or through its direct actions on the M1 and/or H1 receptor. Therefore, to determine

whether the promyelinating effects of clemastine are responsible for behavioural rescue, we tested the efficacy of sobetirome, a promyelinating compound that has an entirely different mechanism of action compared to clemastine. Sobetirome is a thyroid hormone receptor (TR) agonist, and Sob-AM2 is a prodrug of sobetirome that preferentially delivers sobetirome to the CNS from a systemic dose. Both drugs were previously shown to promote OPC differentiation and remyelination in preclinical mouse models of demyelination.<sup>18</sup> Primary OPC cultures were differentiated on DIV7 with OL differentiation media containing either sobetirome (1  $\mu$ M) or vehicle (DMSO) and fed daily with fresh media containing sobetirome or vehicle before immunostaining on DIV14 (Fig. 7A). We performed blinded quantification of OPCs and OLs using antibodies against PDGFR $\alpha$  and MBP, respectively, and normalized our counts with the pan-OL marker OLIG2. Consistent with previous observations,<sup>6</sup>  $Tcf4^{+tr}$  cultures treated with vehicle exhibited a significant decrease in OLs (MBP+/OLIG2+) along with a significant increase in OPCs (PDGFR $\alpha$ +/OLIG2+) when compared to  $Tcf4^{+/+}$  littermate controls (Fig. 7B and C). Sobetirome treatment resulted in a significant reduction in OPCs and an increase in OLs when compared to vehicle-treated  $Tcf4^{+tr}$  cells (Fig. 7B and C). These data indicate sobetirome is effective at overcoming the deleterious effects of  $Tcf4$  mutation on OL development by promoting differentiation of OPCs into OLs, and thereby normalizing the OL population to similar proportions of OPCs and OLs as observed in  $Tcf4^{+/+}$  cultures. Next, we assessed the *in vivo* effectiveness of Sob-AM2 by dosing  $Tcf4^{+tr}$  mice and  $Tcf4^{+/+}$  littermates intraperitoneally with either Sob-AM2 (1 mg/kg) or vehicle for 2 weeks followed by immunohistochemical

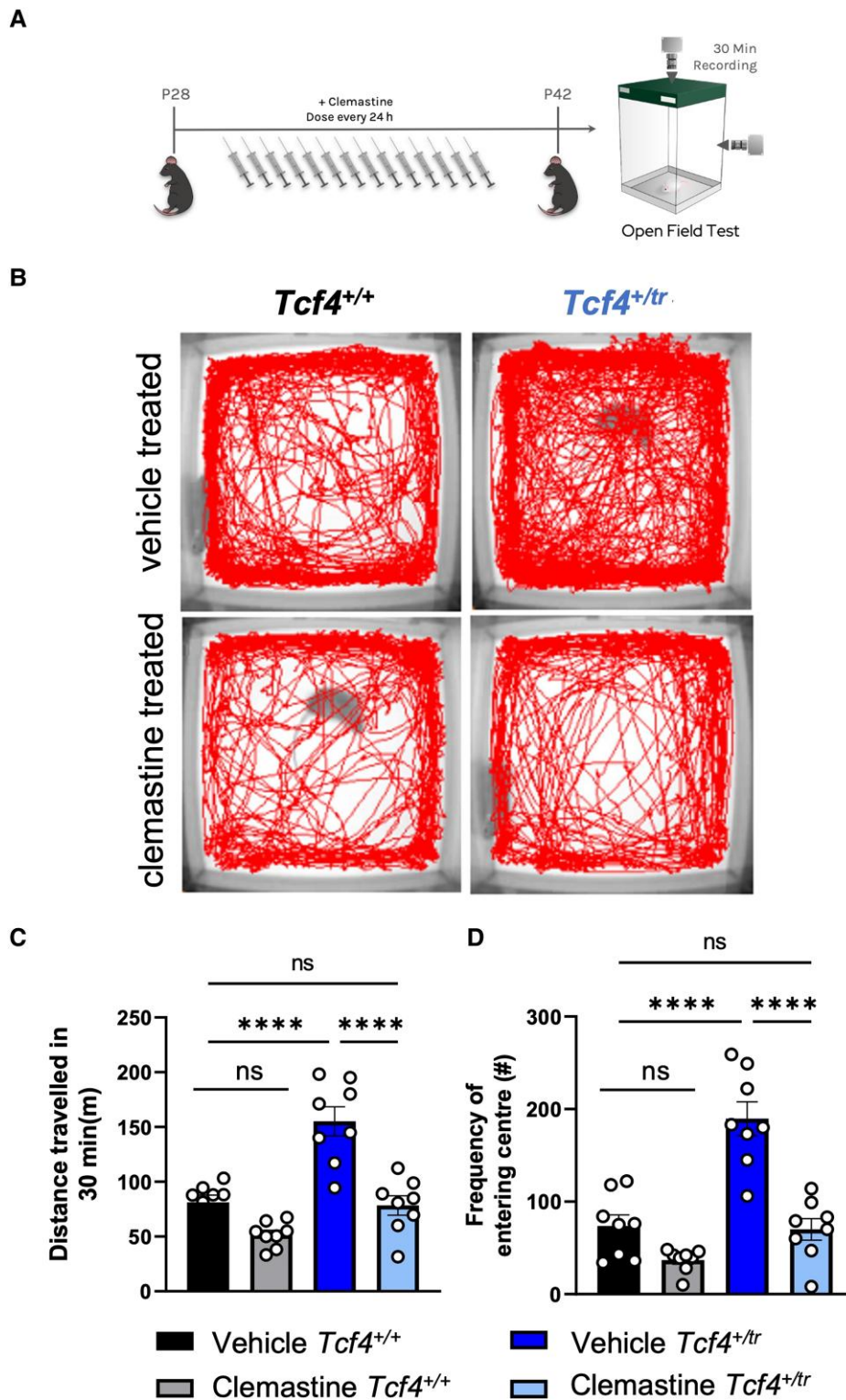


**Figure 6** Clemastine rescues behavioural deficits in *Tcf4*<sup>+/*tr*</sup> mice. (A) Graphical representation of the dosing regime and subsequent behavioural analysis. (B) Locomotor activity maps from *Tcf4*<sup>+/+</sup> and *Tcf4*<sup>+/*tr*</sup> mice treated with vehicle or clemastine for 14 days. Movement was recorded for 30 min following placement in a 37.5 × 37.5 cm novel open field arena. (C) Summary plot showing vehicle-treated *Tcf4*<sup>+/*tr*</sup> mice have hyperlocomotion compared to vehicle-treated *Tcf4*<sup>+/+</sup> mice. Hyperlocomotion is reduced in clemastine-treated *Tcf4*<sup>+/*tr*</sup> mice compared to vehicle-treated *Tcf4*<sup>+/+</sup> mice [two-way ANOVA,  $n = 8$  biologically independent animals/genotype,  $F(1,7) = 20.41$ ,  $P = 0.0027$ , data are presented as mean values ± SEM]. (D) Summary plot showing the frequency of entering the centre (middle 15.25 × 15.25 cm) is increased in vehicle-treated *Tcf4*<sup>+/*tr*</sup> mice compared to vehicle-treated *Tcf4*<sup>+/+</sup> mice. The frequency of entering the centre is reduced in clemastine-treated *Tcf4*<sup>+/*tr*</sup> mice compared to vehicle-treated *Tcf4*<sup>+/+</sup> mice [two-way ANOVA,  $n = 8$  biologically independent animals/genotype,  $F(1,7) = 10.36$ ,  $P = 0.0147$ ]. Centre values represent the mean and error bars are SEM, \*\*\*\* $P < 0.0001$ .

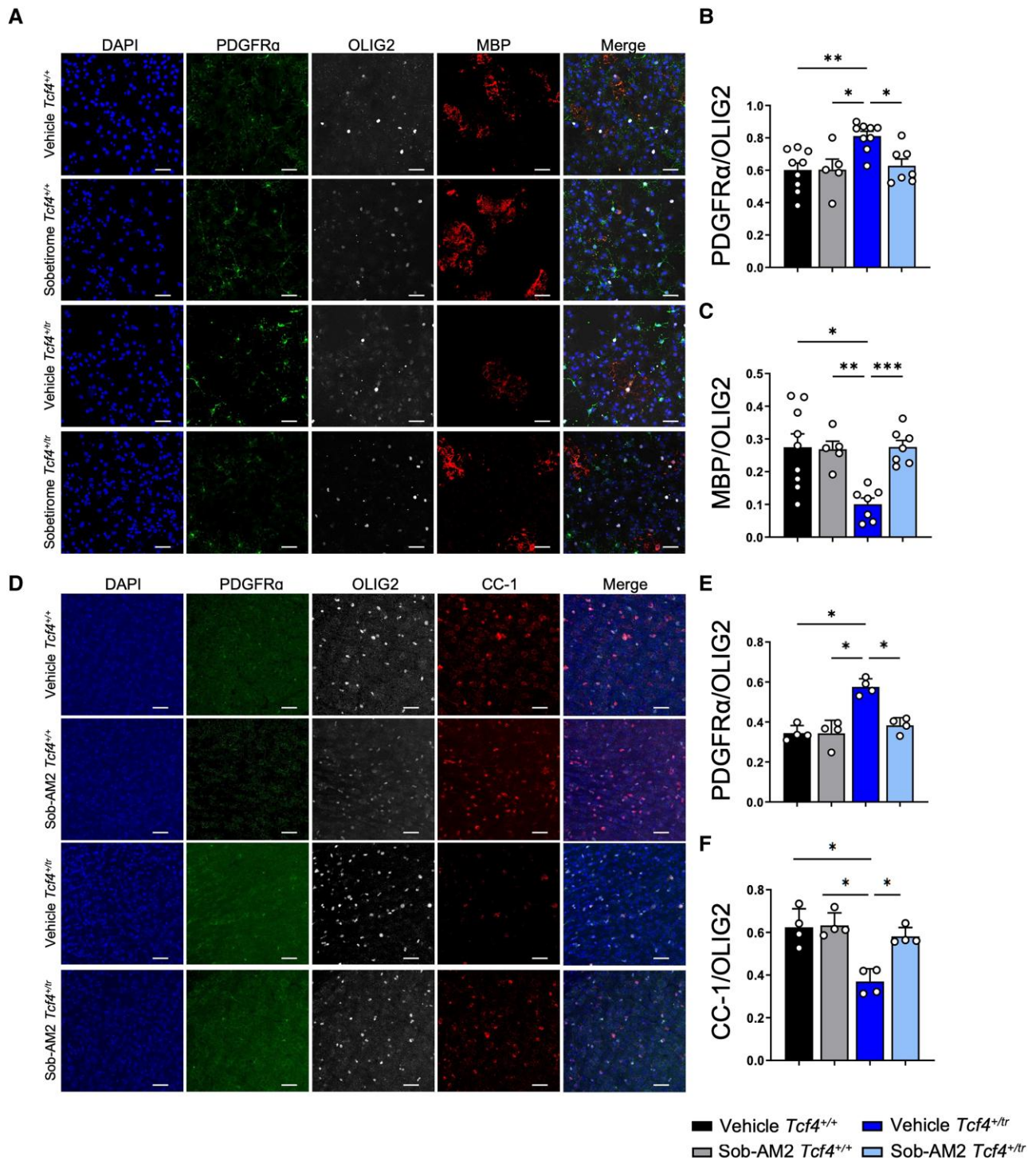


**Figure 7** Sobetirome and Sob-AM2 increase the proportion of OLs both *in vitro* and *in vivo* in *Tcf4*<sup>+tr</sup> mice. (A) Immunocytochemistry of DIV14 OPC/OL cultures following 7-day treatment of either vehicle (DMSO) or sobetirome (1 μM). Cultures stained for DAPI (blue, column 1), PDGFRα (green, column 2), MBP (red, column 4) and OLIG2 (grey, column 3). Scale bars = 50 μm. (B) Summary plot showing increased proportion of PDGFRα/OLIG2 cells in vehicle-treated *Tcf4*<sup>+tr</sup> cultures compared to vehicle-treated *Tcf4*<sup>+/+</sup> cultures. The proportion of PDGFRα/OLIG2 cells in clemastine-treated *Tcf4*<sup>+tr</sup> cultures is reduced compared to vehicle-treated *Tcf4*<sup>+tr</sup> cultures [two-way ANOVA, *n* = 8 biologically independent animals/genotype, *F*(1,7) = 14.36, *P* = 0.0068, data are presented as mean values ± SEM]. (C) Summary plot showing decreased proportion of MBP/OLIG2 cells in vehicle-treated *Tcf4*<sup>+tr</sup> cultures compared to vehicle-treated *Tcf4*<sup>+/+</sup> cultures. The proportion of MBP/OLIG2 cells is increased in clemastine-treated *Tcf4*<sup>+tr</sup> cultures compared to vehicle-treated *Tcf4*<sup>+tr</sup> cultures [two-way ANOVA, *n* = 8 biologically independent animals/genotype, *F*(1,6) = 18.65, *P* = 0.005, data are presented as mean values ± SEM]. (D) Immunohistochemistry of OPC/OL in 55 μm-thick tissue sections following 14-day treatment of either vehicle (DMSO) or Sob-AM2. Tissue stained for DAPI (blue, column 1), PDGFRα (green, column 2), CC-1 (red, column 4) and OLIG2 (grey, column 3). (E) Summary plot showing increased proportion of PDGFRα/OLIG2 cells in vehicle-treated *Tcf4*<sup>+tr</sup> mice compared to vehicle-treated *Tcf4*<sup>+/+</sup> mice. The proportion of PDGFRα/OLIG2 cells in clemastine-treated *Tcf4*<sup>+tr</sup> mice is reduced compared to vehicle-treated *Tcf4*<sup>+tr</sup> mice [two-way ANOVA, *n* = 4 biologically independent animals/genotype, *F*(1,3) = 16.78, *P* = 0.0263, data are presented as mean values ± SEM]. (F) Summary plot showing decreased proportion of CC-1/OLIG2 cells in vehicle-treated *Tcf4*<sup>+tr</sup> mice compared to vehicle-treated *Tcf4*<sup>+/+</sup> mice. The proportion of CC-1/OLIG2 cells is increased in clemastine-treated *Tcf4*<sup>+tr</sup> cultures compared to vehicle-treated *Tcf4*<sup>+tr</sup> cultures [two-way ANOVA, *n* = 4 biologically independent animals/genotype, *F*(1,3) = 15.57, *P* = 0.029, data are presented as mean values ± SEM].

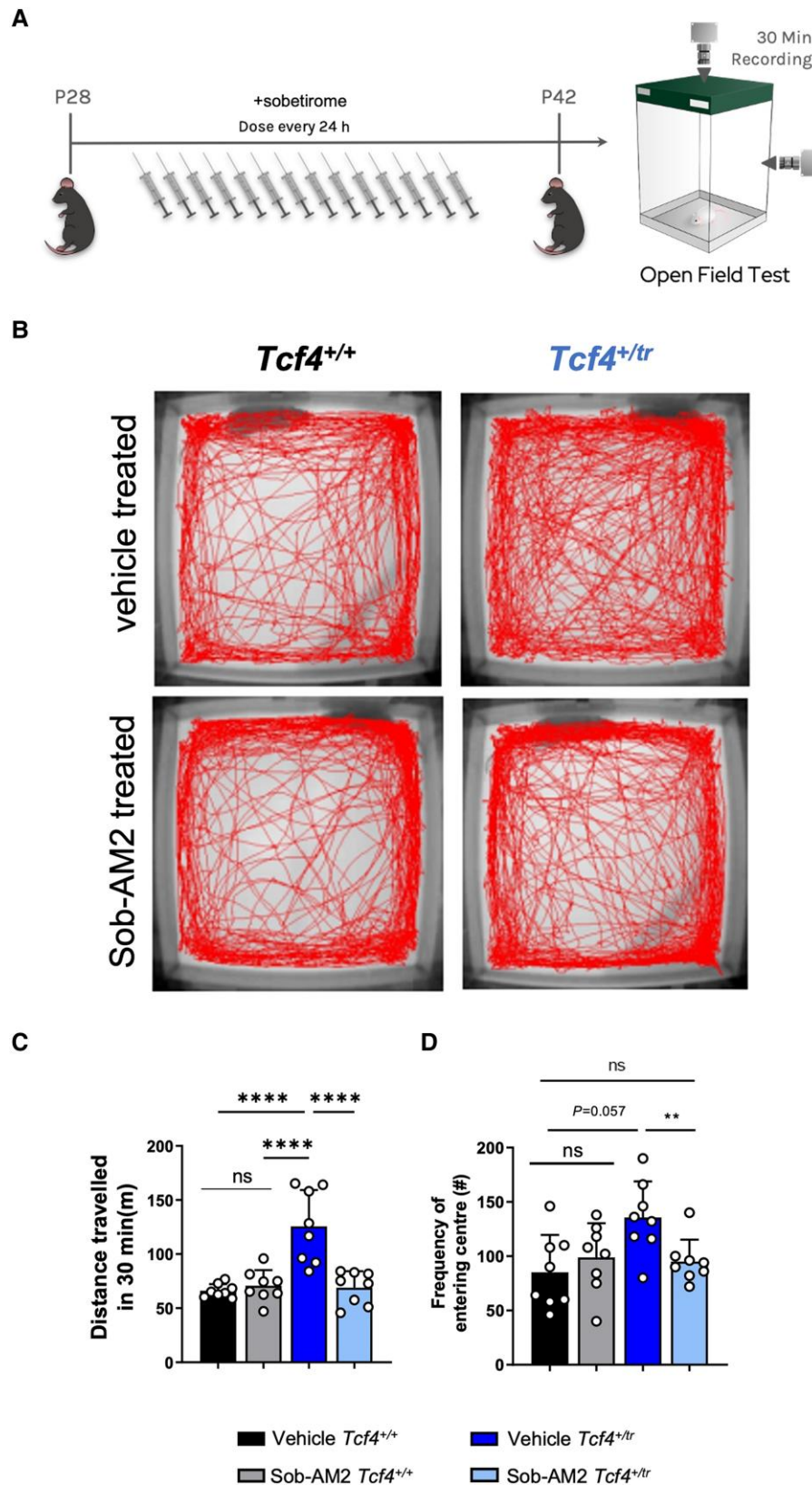


**Figure 8** Sob-AM2 rescues behavioural deficits in *Tcf4*<sup>+tr</sup> mice. (A) Graphical representation of the dosing regime and subsequent behavioural analysis. (B) Locomotor activity maps from *Tcf4*<sup>+/+</sup> and *Tcf4*<sup>+tr</sup> mice treated with vehicle or Sob-AM2 for 14 days. Movement was recorded for 30 min following placement in a 37.5 × 37.5 cm novel open field arena. (C) Summary plot showing vehicle-treated *Tcf4*<sup>+tr</sup> mice have hyperlocomotion compared to vehicle-treated *Tcf4*<sup>+/+</sup> mice. Hyperlocomotion is reduced in Sob-AM2 treated *Tcf4*<sup>+tr</sup> mice compared to vehicle-treated *Tcf4*<sup>+/+</sup> mice [*n* = 8 biologically independent animals/genotype, *F*(1,7) = 7.44, *P* = 0.029, data are presented as mean values ± SEM]. (D) Summary plot showing the frequency of entering the centre (middle 15.25 × 15.25 cm) is increased in vehicle-treated *Tcf4*<sup>+tr</sup> mice compared to vehicle-treated *Tcf4*<sup>+/+</sup> mice. The frequency of entering the centre is reduced in clemastine-treated *Tcf4*<sup>+tr</sup> mice compared to vehicle-treated *Tcf4*<sup>+/+</sup> mice [*n* = 8 biologically independent animals/genotype, *F*(1,7) = 1.22, *P* = 0.305, data are presented as mean values ± SEM]. \*\**P* < 0.01, \*\*\*\**P* < 0.0001.

quantification (Fig. 7D). Consistent with previous results,<sup>6</sup> vehicle-treated  $Tcf4^{+/tr}$  mice showed fewer OLs (CC1+/OLIG2+) and more OPCs (PDGFR $\alpha$ +/OLIG2+) when compared to vehicle-treated  $Tcf4^{+/+}$  littermates (Fig. 7E and F). Similar to our *in vitro* data, Sob-AM2-treated  $Tcf4^{+/tr}$  mice showed a significant increase in OLs that coincided with a significant decrease in OPCs when compared to vehicle-treated  $Tcf4^{+/+}$  littermates (Fig. 7E and F). Together, these data indicate sobetirome and Sob-AM2 are effective both *in vitro* and *in vivo* at promoting OPCs to differentiate into OLs in a mutant  $Tcf4$  background, thereby normalizing the OL population to  $Tcf4^{+/+}$  levels.

Next, we treated  $Tcf4^{+/tr}$  mice and  $Tcf4^{+/+}$  littermates with Sob-AM2 for 14 days and then assayed their behaviour in the open field (Fig. 8A). Vehicle-treated  $Tcf4^{+/tr}$  animals exhibited an overall greater distance travelled and a modest increased frequency of entering the centre of the field (inversely related to anxiety) (Fig. 8B and C). Remarkably, Sob-AM2-treated  $Tcf4^{+/tr}$  mice showed a significant reduction in total distance travelled (Fig. 8C) and reduction in the frequency of entering the centre of the open field (Fig. 8D) compared to vehicle-treated  $Tcf4^{+/tr}$  littermates. These data indicate that Sob-AM2 treatment is effective at normalizing hyperlocomotion and anxiety phenotypes in the PTHS mouse model. All together, these data suggest promyelinating therapies are beneficial to cells, circuits and behaviour in a preclinical model of PTHS, and supports the notion that promyelinating agents could be an applicable therapeutic intervention in humans diagnosed with PTHS.

## Discussion

We have performed a series of experiments to demonstrate that pharmacological enhancement of myelination is effective at normalizing abnormal brain function and behaviour in a mouse model of PTHS. We demonstrated that clemastine, a previously described promyelinating compound, is effective at normalizing OPC and OL density both *in vitro* and *in vivo* (Figs 1 and 2). Additionally, EM analysis showed that clemastine treatment elevated the proportion of uncompact myelin and reduced the g-ratio indicative enhancing the process of myelination (Fig. 3), which was further supported by increases in the proportion of BCAS1 + pre-myelinating OLs (Fig. 4). This enhanced myelination resulted in functional rescue, whereby more CAPs were observed travelling down myelinated axons following treatment with clemastine (Fig. 5). Last, we showed that the clemastine-dependent improvement of OL populations and physiological function occurred in conjunction with normalization of behavioural deficits (Fig. 6). To assess whether clemastine-dependent behavioural recovery was due to enhanced myelination or through direct actions on its receptor targets (H1R and/or M1R), we repeated the *in vitro* and *in vivo* studies with sobetirome and Sob-AM2, which induces OPC differentiation through TR activation.<sup>18</sup> Sobetirome not only increased OLs *in vitro* and *in vivo* (Fig. 7), but also normalized behavioural deficits to a similar degree to clemastine (Fig. 8). Together, these results provide strong evidence that pharmacological enhancement of myelination was responsible for behavioural rescue in the PTHS mouse model and therefore identifies a potential therapeutic approach for PTHS.

### Myelination deficits in Pitt–Hopkins syndrome

Myelination deficits are consistently observed in several different mouse models of PTHS. The initial observation was derived from transcriptomic analysis of five different PTHS mouse models and was subsequently biologically confirmed in the same  $Tcf4^{+/tr}$  mouse model used in this study.<sup>6</sup> Regulation of OL development by  $Tcf4$  was

also shown in the mouse spinal cord where homozygous knockout of the long isoform of  $Tcf4$  resulted in a significant reduction in OLs.<sup>9</sup> Moreover, conditional deletion of  $Tcf4$  in the  $Nkx2.1$  lineage resulted in a significant increase in OPCs of the mouse olfactory bulb.<sup>10</sup>  $Tcf4$  is expressed in all stages of OL development as demonstrated by single cell sequencing and fluorescent *in situ* hybridization, and a cell autonomous effect of  $Tcf4$  on OL phenotypes is established.<sup>6,8–10</sup> Clinical evidence for myelination deficits in PTHS patients is currently qualitative, due to the rare occurrence of this syndrome, with reports of several patients showing delayed myelination, white matter hyperintensities and dysplasia of the CC.<sup>25–29</sup> Future studies using PTHS patient-derived induced pluripotent stem cells will be important to demonstrate whether OL phenotypes observed in the mouse model translate to the human condition.

### Therapeutic potential of clemastine and sobetirome

There are currently no clinically approved therapies that promote myelination.<sup>30,31</sup> The promyelinating capabilities of clemastine were first identified in a drug screen that was specific for functional myelination.<sup>12</sup> Clemastine is an FDA-approved, first-generation antihistamine, that readily crosses the blood–brain barrier; however, its effect on OPCs appears to be through its off-target antimuscarinic effects.<sup>12,16</sup> Clemastine administration has rescued myelination defects in a variety of mouse models of dysmyelination and neurodegeneration, and in a mouse model of Williams Syndrome.<sup>11,15–17,32–35</sup> Moreover, it showed signs of potential efficacy in a phase 2 clinical trial for multiple sclerosis.<sup>36</sup>

Thyroid hormone is a critical signalling molecule that regulates the proliferation and differentiation of OPCs and subsequent development of myelination through its activation of TRs found in OPCs.<sup>37–39</sup> Sobetirome is a clinical-stage TR agonist that is shown to promote myelin repair in clinical models of demyelination.<sup>18,30</sup> Importantly, sobetirome does not show any adverse side effects associated with excess thyroid hormone because of its unique tissue distribution and specificity for TR $\beta$  over TR $\alpha$  receptors.<sup>40–42</sup> The sobetirome prodrug Sob-AM2 is better able to cross the blood–brain barrier and distribute to the CNS following systemic administration, making it suitable for clinical evaluation in demyelinating diseases.<sup>42,43</sup>

Here, we demonstrate that both clemastine and sobetirome/Sob-AM2 are effective at rescuing myelination deficits and behaviour in a mouse model of PTHS. Consistent with previous findings, our results suggest the cellular mechanism for the effect of these compounds is through promoting OPCs to differentiate, as we showed that both compounds shift the OL population by reducing OPCs and increasing OLs (Figs 1, 2 and 7). Clemastine is a H1R antagonist and its effect on OPC differentiation is proposed to work through M1R antagonism,<sup>12–14</sup> whereas sobetirome promotes myelination through activation of TRs. We reason that because these two compounds promote myelination through two different modes of action (i.e. M1R or TR), it therefore indicates the mechanisms underlying behavioural rescue is through their common ability to promote myelination. Moreover, these results also suggest that any promyelinating compound will probably be effective at normalizing behaviour in a PTHS mouse model, and therefore greatly improves the chance of developing a promyelinating therapeutic that will be efficacious and compatible with PTHS patients.

### Myelination deficits in autism spectrum disorder

Evidence for myelination defects across the autism spectrum is building and promyelinating therapies could be a potential therapeutic

target when deficits in myelination are suspected. We previously found that convergent differentially expressed genes across three syndromic ASD mouse models (*Tcf4*, *Mecp2* and *Pten*) were enriched for biological terms related to OLs and myelination.<sup>6</sup> Importantly, the eigengene of these overlapping differentially expressed genes could be used to separate idiopathic ASD cases from controls in a large sample of human post-mortem ASD brains. Moreover, cellular deconvolution of these same post-mortem ASD samples predicted an overall reduction in OL fraction of RNA, suggesting there may be a reduction in OLs in idiopathic ASD.<sup>6</sup> Reanalysis of single cell sequencing data from 41 post-mortem ASD and control brains also identified a reduction in OL abundance.<sup>6,44</sup> In addition, many identified ASD risk genes are known to regulate development and function of cells in the OL lineage. For instance, *SCN2a*, which is considered a high confidence syndromic ASD gene<sup>45,46</sup> is expressed in OPCs and regulates their excitability and development.<sup>47,48</sup> Other high confidence ASD risk genes such as *CHD8*,<sup>49–52</sup> *ADNP*,<sup>53</sup> *PTEN*<sup>54–56</sup> and *POGZ*<sup>57</sup> to name a few, have also been shown to regulate the OL lineage and/or display abnormal myelination in the patient population. The process of myelination temporally coincides with the progression of ASD and immediately precedes the first appearances of the disorder.<sup>19</sup> In addition, it was shown that ongoing myelination is a requirement for long-term consolidation of spatial memory and motor learning in several mouse models,<sup>58–60</sup> which suggests abnormal developmental myelination could underlie intellectual disability and motor deficits, which are common comorbidities in ASD. Fortunately, OPCs are the most abundant proliferating cell population in the human brain and are present throughout the lifespan, which makes them suitable therapeutic targets for NDDs. All together these studies strongly support the concept of enhancing myelination as a potential treatment for not only PTHS, but potentially many subtypes of NDDs and ASDs that are predicted or shown to have myelination delays or deficits.

## Acknowledgements

We are grateful for the vision and generosity of the Lieber and Maltz families, who made this work possible. We thank the Johns Hopkins School of Medicine Microscope Core Facility and specifically LaToya Roker and Michael Delannoy for generating TEM images of CC used in this study.

## Funding

This work was supported by the Lieber Institute, the Pitt–Hopkins Research Foundation Award (B.J.M.), NIMH grant R01MH110487 (B.J.M.), and NHLBI grant R01HL104101 and R01HL137094 (D.K.M.). The content is solely the responsibility of the authors and does not necessarily represent the official views of the National Institutes of Health.

## Competing interests

T.S.S. is a founder and adviser to Autobahn Therapeutics. T.S.S. and T.B. are inventors of licensed patent applications claiming CNS-penetrating thymomimetics. All other authors declare no competing interests.

## Supplementary material

Supplementary material is available at *Brain* online.

## References

- Chen H-Y, Bohlen JF, Maher BJ. Molecular and cellular function of transcription factor 4 in Pitt-Hopkins syndrome. *Dev Neurosci*. 2021;43:159–167.
- Thaxton C, Kloth AD, Clark EP, Moy SS, Chitwood RA, Philpot BD. Common pathophysiology in multiple mouse models of Pitt-Hopkins syndrome. *J Neurosci*. 2018;38:918–936.
- Cleary CM, James S, Maher BJ, Mulkey DK. Disordered breathing in a Pitt-Hopkins syndrome model involves *Phox2b*-expressing parafacial neurons and aberrant *Nav1.8* expression. *Nat Commun*. 2021;12:5962.
- Grubišić V, Kennedy AJ, Sweatt JD, Parpura V. Pitt-Hopkins mouse model has altered particular gastrointestinal transits in vivo. *Autism Res*. 2015;8:629–633.
- Kennedy AJ, Rahn EJ, Paulukaitis BS, et al. *Tcf4* regulates synaptic plasticity, DNA methylation, and memory function. *Cell Rep*. 2016;16:2666–2685.
- Phan BN, Bohlen JF, Davis BA, et al. A myelin-related transcriptomic profile is shared by Pitt-Hopkins syndrome models and human autism spectrum disorder. *Nat Neurosci*. 2020;23:375–385.
- Kim H, Berens NC, Ochandarena NE, Philpot BD. Region and cell type distribution of *TCF4* in the postnatal mouse brain. *Front Neuroanat*. 2020;14:42.
- Marques S, Zeisel A, Codeluppi S, et al. Oligodendrocyte heterogeneity in the mouse juvenile and adult central nervous system. *Science*. 2016;352:1326–1329.
- Wedel M, Fröb F, Elsesser O, et al. Transcription factor *Tcf4* is the preferred heterodimerization partner for *Olig2* in oligodendrocytes and required for differentiation. *Nucleic Acids Res*. 2020;48:4839–4857.
- Zhang X, Huang N, Xiao L, Wang F, Li T. Replenishing the aged brains: Targeting oligodendrocytes and myelination? *Front Aging Neurosci*. 2021;13:760200.
- Lee JI, Park JW, Lee KJ, Lee DH. Clemastine improves electrophysiological and histomorphometric changes through promoting myelin repair in a murine model of compression neuropathy. *Sci Rep*. 2021;11:20886.
- Mei F, Fancy SPJ, Shen Y-AA, et al. Micropillar arrays as a high-throughput screening platform for therapeutics in multiple sclerosis. *Nat Med*. 2014;20:954–960.
- Chen J-F, Liu K, Hu B, et al. Enhancing myelin renewal reverses cognitive dysfunction in a murine model of Alzheimer's disease. *Neuron*. 2021;109:2292–2307.e5.
- Minigh J. Clemastine. In: *XPharm: The comprehensive pharmacology reference*. Elsevier; 2008:1–6.
- Li Z, He Y, Fan S, Sun B. Clemastine rescues behavioral changes and enhances remyelination in the cuprizone mouse model of demyelination. *Neurosci Bull*. 2015;31:617–625.
- Mei F, Lehmann-Horn K, Shen Y-AA, et al. Accelerated remyelination during inflammatory demyelination prevents axonal loss and improves functional recovery. *eLife*. 2016;5:e18246.
- Liu J, Dupree JL, Gacias M, et al. Clemastine enhances myelination in the prefrontal cortex and rescues behavioral changes in socially isolated mice. *J Neurosci*. 2016;36:957–962.
- Hartley MD, Banerji T, Tagge IJ, et al. Myelin repair stimulated by CNS-selective thyroid hormone action. *JCI Insight*. 2019;4:e126329.
- Deoni SCL, Zinkstok JR, Daly E, et al. White-matter relaxation time and myelin water fraction differences in young adults with autism. *Psychol Med*. 2015;45:795–805.
- Yoshida A, Takashima K, Shimonaga T, Kadokura M, Nagase S, Koda S. Establishment of a simple one-step method for oligodendrocyte progenitor cell preparation from rodent brains. *J Neurosci Methods*. 2020;342:108798.

21. Maher BJ, LoTurco JJ. Disrupted-in-schizophrenia (DISC1) functions presynaptically at glutamatergic synapses. *PLoS ONE*. 2012;7:e34053.
22. Mickelsen LE, Bolisetty M, Chimileski BR, et al. Single-cell transcriptomic analysis of the lateral hypothalamic area reveals molecularly distinct populations of inhibitory and excitatory neurons. *Nat Neurosci*. 2019;22:642–656.
23. Olmos-Serrano JL, Kang HJ, Tyler WA, et al. Down syndrome developmental brain transcriptome reveals defective oligodendrocyte differentiation and myelination. *Neuron*. 2016;89:1208–1222.
24. Ekins S, Puhl AC, Davidow A. Repurposing the dihydropyridine calcium channel inhibitor nifedipine as a nav1.8 inhibitor in vivo for Pitt Hopkins syndrome. *Pharm Res*. 2020;37:127.
25. Amiel J, Rio M, de Pontual L, et al. Mutations in TCF4, encoding a class I basic helix-loop-helix transcription factor, are responsible for Pitt-Hopkins syndrome, a severe epileptic encephalopathy associated with autonomic dysfunction. *Am J Hum Genet*. 2007;80:988–993.
26. Goodspeed K, Newsom C, Morris MA, Powell C, Evans P, Golla S. Pitt-Hopkins syndrome: A review of current literature, clinical approach, and 23-patient case series. *J Child Neurol*. 2018;33:233–244.
27. Rosenfeld JA, Leppig K, Ballif BC, et al. Genotype-phenotype analysis of TCF4 mutations causing Pitt-Hopkins syndrome shows increased seizure activity with missense mutations. *Genet Med*. 2009;11:797–805.
28. Brockschmidt A, Filippi A, Charbel Issa P, et al. Neurologic and ocular phenotype in Pitt-Hopkins syndrome and a zebrafish model. *Hum Genet*. 2011;130:645–655.
29. Stavropoulos DJ, MacGregor DL, Yoon G. Mosaic microdeletion 18q21 as a cause of mental retardation. *Eur J Med Genet*. 2010;53:396–399.
30. Hartley MD, Altowajri G, Bourdette D. Remyelination and multiple sclerosis: Therapeutic approaches and challenges. *Curr Neurol Neurosci Rep*. 2014;14:485.
31. Plemel JR, Liu W-Q, Yong VW. Remyelination therapies: A new direction and challenge in multiple sclerosis. *Nat Rev Drug Discov*. 2017;16:617–634.
32. Xie Y-Y, Pan T-T, Xu D-E, et al. Clemastine ameliorates myelin deficits via preventing senescence of oligodendrocyte precursor cells in Alzheimer's disease model mouse. *Front Cell Dev Biol*. 2021;9:733945.
33. Barak B, Zhang Z, Liu Y, et al. Neuronal deletion of Gtf2i, associated with Williams syndrome, causes behavioral and myelin alterations rescuable by a remyelinating drug. *Nat Neurosci*. 2019;22:700–708.
34. Deshmukh VA, Tardif V, Lyssiotis CA, et al. A regenerative approach to the treatment of multiple sclerosis. *Nature*. 2013;502:327–332.
35. Cree BAC, Niu J, Hoi KK, et al. Clemastine rescues myelination defects and promotes functional recovery in hypoxic brain injury. *Brain*. 2018;141:85–98.
36. Green AJ, Gelfand JM, Cree BA, et al. Clemastine fumarate as a remyelinating therapy for multiple sclerosis (ReBUILD): A randomised, controlled, double-blind, crossover trial. *Lancet*. 2017;390:2481–2489.
37. Barres BA, Lazar MA, Raff MC. A novel role for thyroid hormone, glucocorticoids and retinoic acid in timing oligodendrocyte development. *Development*. 1994;120:1097–1108.
38. Gao FB, Apperly J, Raff M. Cell-intrinsic timers and thyroid hormone regulate the probability of cell-cycle withdrawal and differentiation of oligodendrocyte precursor cells. *Dev Biol*. 1998;197:54–66.
39. Billon N, Jolicoeur C, Tokumoto Y, Vennström B, Raff M. Normal timing of oligodendrocyte development depends on thyroid hormone receptor alpha 1 (TRalpha1). *EMBO J*. 2002;21:6452–6460.
40. Scanlan TS. Sobetirome: A case history of bench-to-clinic drug discovery and development. *Heart Fail Rev*. 2010;15:177–182.
41. Ferrara SJ, Meinig JM, Placzek AT, et al. Ester-to-amide rearrangement of ethanolamine-derived prodrugs of sobetirome with increased blood-brain barrier penetration. *Bioorg Med Chem*. 2017;25:2743–2753.
42. Placzek AT, Ferrara SJ, Hartley MD, Sanford-Crane HS, Meinig JM, Scanlan TS. Sobetirome prodrug esters with enhanced blood-brain barrier permeability. *Bioorg Med Chem*. 2016;24:5842–5854.
43. Manzano J, Morte B, Scanlan TS, Bernal J. Differential effects of triiodothyronine and the thyroid hormone receptor beta-specific agonist GC-1 on thyroid hormone target genes in the brain. *Endocrinology*. 2003;144:5480–5487.
44. Velmeshev D, Schirmer L, Jung D, et al. Single-cell genomics identifies cell type-specific molecular changes in autism. *Science*. 2019;364:685–689.
45. Fu JM, Satterstrom FK, Peng M, et al. Rare coding variation illuminates the allelic architecture, risk genes, cellular expression patterns, and phenotypic context of autism. *medRxiv*. Published online December 21, 2021.
46. Satterstrom FK, Kosmicki JA, Wang J, et al. Large-scale exome sequencing study implicates both developmental and functional changes in the neurobiology of autism. *Cell*. 2020;180:568–584.e23.
47. Berret E, Barron T, Xu J, Debner E, Kim EJ, Kim JH. Oligodendroglial excitability mediated by glutamatergic inputs and Nav1.2 activation. *Nat Commun*. 2017;8:557.
48. Gould E, Kim JH. SCN2A contributes to oligodendroglia excitability and development in the mammalian brain. *Cell Rep*. 2021;36:109653.
49. Marie C, Clavairoly A, Frah M, et al. Oligodendrocyte precursor survival and differentiation requires chromatin remodeling by Chd7 and Chd8. *Proc Natl Acad Sci U S A*. 2018;115:E8246–E8255.
50. Jung H, Park H, Choi Y, et al. Sexually dimorphic behavior, neuronal activity, and gene expression in Chd8-mutant mice. *Nat Neurosci*. 2018;21:1218–1228.
51. Zhao C, Dong C, Frah M, et al. Dual requirement of CHD8 for chromatin landscape establishment and histone methyltransferase recruitment to promote CNS myelination and repair. *Dev Cell*. 2018;45:753–768.e8.
52. Kawamura A, Katayama Y, Nishiyama M, et al. Oligodendrocyte dysfunction due to Chd8 mutation gives rise to behavioral deficits in mice. *Hum Mol Genet*. 2020;29:1274–1291.
53. Van Dijck A, Vulto-van Silfhout AT, Cappuyns E, et al. Clinical presentation of a complex neurodevelopmental disorder caused by mutations in ADNP. *Biol Psychiatry*. 2019;85:287–297.
54. Tilot AK, Gaugler MK, Yu Q, et al. Germline disruption of Pten localization causes enhanced sex-dependent social motivation and increased glial production. *Hum Mol Genet*. 2014;23:3212–3227.
55. Frazier TW, Embacher R, Tilot AK, Koenig K, Mester J, Eng C. Molecular and phenotypic abnormalities in individuals with germline heterozygous PTEN mutations and autism. *Mol Psychiatry*. 2015;20:1132–1138.
56. Goebbels S, Oltrogge JH, Kemper R, et al. Elevated phosphatidylinositol 3,4,5-trisphosphate in glia triggers cell-autonomous membrane wrapping and myelination. *J Neurosci*. 2010;30:8953–8964.

57. Suliman-Lavie R, Title B, Cohen Y, et al. Pogz deficiency leads to transcription dysregulation and impaired cerebellar activity underlying autism-like behavior in mice. *Nat Commun.* 2020; 11:5836.
58. Steadman PE, Xia F, Ahmed M, et al. Disruption of oligodendrogenesis impairs memory consolidation in adult mice. *Neuron.* 2020;105:150-164.e6.
59. McKenzie IA, Ohayon D, Li H, et al. Motor skill learning requires active central myelination. *Science.* 2014;346:318-322.
60. Pan Y, Cai K, Cheng M, Zou X, Li M. Responsive social smile: A machine learning based multimodal behavior assessment framework towards early stage autism screening. In: 2020 25th International Conference on Pattern Recognition (ICPR). IEEE; 2021:2240-2247.